

## Propagating convection fronts

M. Lücke

*Institut für Theoretische Physik, Universität des Saarlandes, D-6600 Saarbrücken, West Germany  
and Institut für Festkörperforschung, Kernforschungsanlage Jülich, D-5170 Jülich, West Germany*

M. Mihelcic and B. Kowalski

*Institut für Festkörperforschung, Kernforschungsanlage Jülich, D-5170 Jülich, West Germany  
(Received 22 September 1986)*

The evolution of periodic patterns of parallel convective rolls in a fluid heated from below that grow inwards from a sidewall after applying a lateral heat pulse is determined from numerical solutions of the Oberbeck-Boussinesq equations. Propagation speed and intensity profile of the front between homogeneous conductive and periodic convective state and the wave number selected under the front are determined for several Rayleigh numbers.

In many dissipative systems spatially periodic structures grow out of a homogeneous basic state when the driving exceeds a critical value. If the level of imperfections that break the system's translational invariance is fairly uniform then the periodic state grows globally after increasing the driving from a subcritical to a supercritical value. Here we investigate a situation<sup>1-4</sup> where the periodic structure is generated initially only in a small spatial region after a setup to supercritical driving, e.g., by a local perturbation applied for a short time. Then the stable periodic state expands into the remaining space that is, in the absence of sizable imperfections, still occupied by the now unstable homogeneous state. This can result in a front between the two states propagating with stationary speed, shape, and spatial intensity profile.<sup>3,4</sup>

In this Rapid Communication we show that in a fluid layer heated from below a convective roll pattern expanding into the quiescent fluid does form such a front. Moreover, for small deviations,  $\varepsilon = R/R_c - 1$ , of the Rayleigh number  $R$  from the critical one,  $R_c$ , for onset of convection the front propagation speed  $c$  agrees very well with the one,  $c_A \sim \sqrt{\varepsilon}$ , obtained<sup>5</sup> from a Ginzburg-Landau-type amplitude equation.<sup>6</sup> Also the spatial extension  $l$  of the front agrees fairly well with the result of the amplitude equation,  $l_A \sim 1/\sqrt{\varepsilon}$ , in the driving range  $0.01 \lesssim \varepsilon \lesssim 0.2$  investigated here. The spatial structure of the roll pattern selected by and evolving under the propagating front is for small  $\varepsilon$  determined by that wave number of perturbations of the conductive state which grows fastest.

These results were obtained by numerically solving the full two-dimensional Oberbeck-Boussinesq equations for a fluid of Prandtl number  $\sigma = 1$  with realistic, i.e., standard experimental boundary conditions in a rectangular  $x$ - $z$  plane of a box of height  $d$  in  $z$  direction and length  $L = 25d$  in  $x$  direction. We used an explicit finite-difference method<sup>7</sup> with a spatial resolution of  $0.05d$  and a time step of  $5 \times 10^{-4} \tau$ . Here  $\tau = d^2/\kappa$  is the characteristic vertical heat diffusion time. Convection fronts traveling inwards from a box wall were generated in the following experimentally reproducible procedure: Starting from a stationary subcritical conductive state with a quiescent

fluid the temperature at the bottom plate,  $z = 0$ , of the box was suddenly increased to a supercritical value corresponding to a small  $\varepsilon > 0$ . For a duration of  $0.2\tau$  after the step, the vertical boundary at  $x = L$  was heated uniformly by imposing a localized horizontal temperature gradient. Thereafter this box wall was a no-slip thermal insulator with zero horizontal heat flux being enforced at  $x = L$ . We also simulated<sup>7</sup> sidewalls that were thermally attached to either the top or the bottom plate and found different transients but no difference in the final stationary front propagation. Since  $x = 0$  was set up to be a mirror plane we, in fact, simulated a box  $-L \leq x \leq L$  with fronts moving inwards symmetrically from the "real" ends at  $\pm L$ .

The above heat pulse entering into the fluid horizontally through the sidewalls initiates convection close to the sidewalls while in the bulk of the box the quiescent conductive state, though being unstable for  $\varepsilon > 0$ , still prevails due to a lack of sizable imperfections that trigger convective growth. (To be precise, the conductive temperature profile in the bulk adjusts diffusively to the new temperature of the bottom plate on a time scale of  $\tau$  after the stepup.) Then the convection state invades the conductive state starting from a sidewall as can be seen from Fig. 1. There we show typical vertical velocity fields  $w(x)$ , which are a signature of convection, at midheight,  $z = d/2$ , at different times after the stepup. The intensity profiles of  $w(x)$  at other vertical positions evolve in the same way so that the convective front propagating inward is aligned parallel to the sidewall at  $x = L$ . Note that the convection rolls indicated schematically in the lower part of Fig. 1 practically do not move. Only the envelope profile of the spatial oscillations of the fields of velocity, temperature, and pressure moves. The final state far behind the front is stationary and of uniform amplitude except for the weaker convective rolls near the thermally insulating sidewalls.

To analyze the velocity and the intensity profile of the front we determined at successive times the positions in the front where the convective flow has reached given fractions  $\alpha$  of the final bulk flow intensity. These front intensity positions marked in Fig. 1 by a cross ( $\alpha = 0.1$ ), a circle ( $\alpha = 0.25$ ), and a triangle ( $\alpha = 0.5$ ) move piecewise

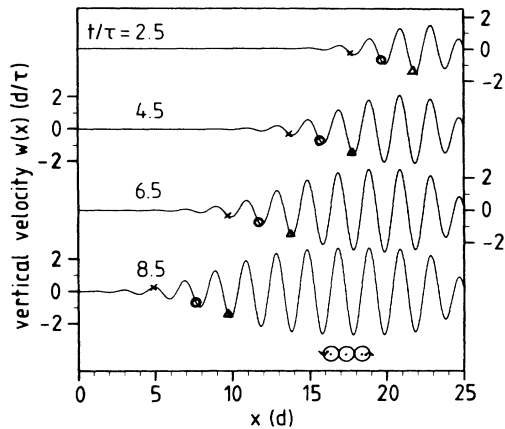


FIG. 1. Vertical convective velocity field  $w(x)$  at midheight  $z=d/2$  at different times after the stepup to  $\varepsilon=0.05$ . Zero crossings mark the centers of the convective rolls, positive (negative)  $w$  implies up (down) flow as indicated in the schematic cross sections of the rolls shown in the lower part of the figure. The front positions where the flow has reached the fraction  $\alpha$  of the final bulk intensity are denoted by a cross for  $\alpha=0.1$ , by a circle for  $\alpha=0.25$ , and by a triangle for  $\alpha=0.5$ .

continuously. The discontinuity of roughly a roll diameter occurs whenever the next vortex ahead reaches the assigned intensity level.

Figure 2 shows the trajectories of the above three front intensity positions as a function of time. After initial transients have died out rather quickly the convection front travels with constant speed  $c$  and with a stationary envelope profile: Relative distances between different front intensity positions do not change any more. However, when the front arrives at the boundary at  $x=0$  (around  $11\tau$  in Fig. 2) the trajectories of the intensity positions level off. Note that this convective front propaga-

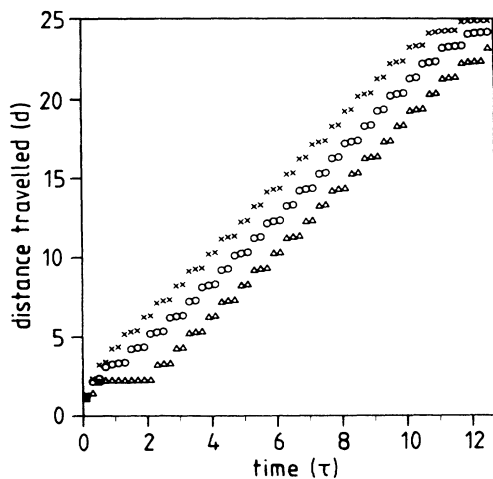


FIG. 2. Front intensity positions (cf. Fig. 1) vs time. Distances traveled by the front positions at which the flow reached a fraction  $\alpha$  of the final bulk intensity are shown for  $\alpha=0.1$  (crosses),  $\alpha=0.25$  (circles), and  $\alpha=0.5$  (triangles).

tion can be observed in experiments if, after a stepup in driving, the time for imperfection-triggered onset of convection which competes with sidewall heating initiated convection is longer than the traveling time of the front. Thus, to observe a front traveling, e.g., over a distance of  $15d$  at  $\varepsilon=0.05$  the above onset time should exceed seven vertical diffusion times which seems to be achievable with well machined apparatus.

The front extension  $l$  as well as the propagation speed  $c$  depends on the supercritical driving  $\varepsilon$ . Figure 3 shows that the stationary convective front propagation speeds in the driving range  $0.01 \lesssim \varepsilon \lesssim 0.2$  are very close to the front velocity

$$c_A = 2\sqrt{\varepsilon}\xi_0/\tau_0, \quad (1)$$

obtained<sup>5</sup> from the special propagating real solution<sup>8</sup>

$$A(x,t) = \sqrt{\varepsilon}f(\sqrt{\varepsilon}x/\xi_0 - 2\varepsilon t/\tau_0) \quad (2)$$

of the amplitude equation

$$\tau_0\partial_t A = (\xi_0^2\partial_x^2 + \varepsilon - |A|^2)A. \quad (3)$$

The scales  $\xi_0=0.385d$  and  $\tau_0=\tau/13$  follow from a linear analysis<sup>9</sup> of the conductive state's stability against growth of straight parallel rolls in laterally infinite boxes. Equation (3) describes at order  $\sqrt{\varepsilon}$  slow variations of the amplitude of, e.g., the vertical velocity field

$$w(x,t) = \text{const} \times \text{Re}[A(x,t)e^{ik_c x}]$$

at midheight,  $z=d/2$ , of the box with  $k_c=3.116/d$  being the critical wave number of rolls at onset of convection. Now, Aronson and Weinberger<sup>5</sup> have shown that a very wide class of real initial amplitude profiles  $A(x,t_0)/\sqrt{\varepsilon}$  that vary between 0 and 1 evolve under Eq. (3) into a unique profile  $f(\zeta)$  (2) propagating with velocity  $c_A$  (1).

The front extension,  $l_A$ , of this profile<sup>4</sup> measured, e.g.,

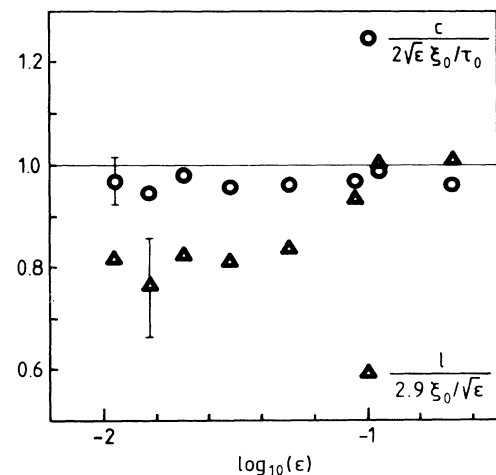


FIG. 3. Stationary velocity  $c$  and spatial extension  $l$  of propagating convective fronts as a function of driving. Values and error bars were obtained from space-time diagrams like Fig. 1 with  $l$  being the distance between the 0.1 and 0.5 front intensity positions. The line corresponds to the result  $c_A$  (1) and  $l_A$  (4) of the amplitude equation.

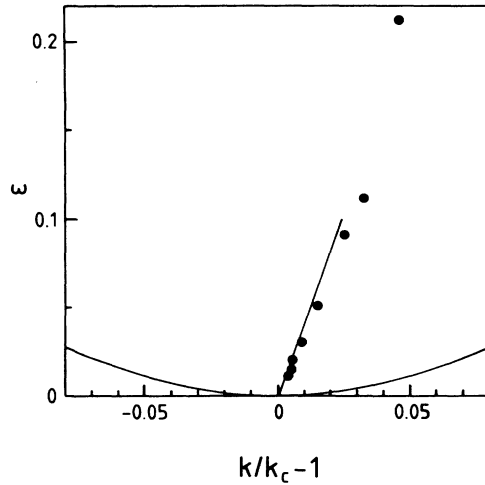


FIG. 4. Wave number selected by the front as a function of driving. The filled circles denote the wave number measured in the stationary propagation mode at the 0.1 front intensity positions (cross in Fig. 1). The straight line represents wave numbers with fastest growth obtained (Ref. 9) from a linear stability analysis of the conductive state at  $R_c$ . The parabola is the Eckhaus stability boundary (Ref. 10) of the convective roll state.

by the distance between the 0.1 and 0.5 intensity level is

$$l_A = 2.9\xi_0/\sqrt{\varepsilon}. \quad (4)$$

The convective front profiles determined from the solution of the full Oberbeck-Boussinesq equations, on the other hand, are somewhat more compressed as can be seen from the triangles in Fig. 3.

Last we show in Fig. 4 the wave numbers of the roll pattern selected by the propagating front as a function of driving. At small  $\varepsilon$  they are given by the wave numbers<sup>9</sup>  $k_{\max}/k_c = 1 + 0.245\varepsilon$  of perturbations of the conductive state which have the largest growth rate for  $\varepsilon \rightarrow 0$ .

The convective fronts described here have many properties in common<sup>7</sup> with fronts formed by toroidal Taylor vortices growing into unstable circular Couette flow between concentric cylinders.

*Note added in proof.* After submission of this paper, experimentally observed convection fronts have been reported<sup>11</sup> that were generated by sidewall heating. The propagation velocity was  $c_A$ . The selected wave number differed from  $k_c$  due to the special design of the experimental cell.

This work was supported by the Stiftung Volkswagenwerk.

<sup>1</sup>J. S. Langer, *Rev. Mod. Phys.* **52**, 1 (1980).

<sup>2</sup>G. I. Sivashinsky, *Annu. Rev. Fluid Mech.* **15**, 179 (1983).

<sup>3</sup>G. Ahlers and D. S. Cannell, *Phys. Rev. Lett.* **50**, 1583 (1983).

<sup>4</sup>M. Lücke, M. Mihelcic, and K. Wingerath, *Phys. Rev. Lett.* **52**, 625 (1984); *Phys. Rev. A* **31**, 396 (1985).

<sup>5</sup>D. G. Aronson and H. F. Weinberger, *Advances in Mathematics* (Academic, New York, 1978), Vol. 30, p. 33.

<sup>6</sup>L. A. Segel, *J. Fluid Mech.* **38**, 203 (1969); A. C. Newell and J. A. Whitehead, *ibid.* **38**, 279 (1969).

<sup>7</sup>M. Lücke, M. Mihelcic, B. Kowalski, and K. Wingerath, *The*

*Physics of Structure Formation: Theory and Simulation*, edited by W. Güttinger and G. Dangelmayr, Springer Series in Synergetics (Springer, Berlin, 1987).

<sup>8</sup>G. Dee and J. S. Langer, *Phys. Rev. Lett.* **50**, 383 (1983).

<sup>9</sup>M. A. Dominguez-Lerma, G. Ahlers, and D. S. Cannell, *Phys. Fluids* **27**, 856 (1984).

<sup>10</sup>W. Eckhaus, *Studies in Nonlinear Stability Theory* (Springer, New York, 1965).

<sup>11</sup>J. Fineberg and V. Steinberg, *Phys. Rev. Lett.* **58**, 1332 (1987).